Environmental Pollution 308 (2022) 119713

Contents lists available at ScienceDirect

Environmental Pollution

journal homepage: www.elsevier.com/locate/envpol

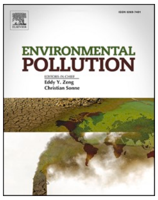

Atmospheric occurrences of nitrated and hydroxylated polycyclic aromatic hydrocarbons from typical e-waste dismantling sites☆

Shengtao Ma[a,b,c], Haojia Chen[a,b], Congcong Yue[a,b], Ranran Liu[a,b], Jian Tang[a,b], Meiqing Lin[a,b], Guiying Li[a,b], Yan Yang[a,b,c], Yingxin Yu[a,b], Taicheng An[a,b,d,*]

[a] *Guangdong-Hong Kong-Macao Joint Laboratory for Contaminants Exposure and Health, Guangdong Key Laboratory of Environmental Catalysis and Health Risk Control, Institute of Environmental Health and Pollution Control, Guangdong University of Technology, Guangzhou, 510006, China*

[b] *Guangdong Engineering Technology Research Center for Photocatalytic Technology Integration and Equipment, Guangzhou Key Laboratory of Environmental Catalysis and Pollution Control, School of Environmental Science and Engineering, Guangdong University of Technology, Guangzhou, 510006, China*

[c] *Synergy Innovation Institute of GDUT, Shantou, 515041, China*

[d] *Chemistry and Chemical Engineering Guangdong Laboratory, Shantou, 515031, China*

ARTICLE INFO

Keywords:
Nitrated PAHs
Hydroxylated PAHs
Electronic waste dismantling
Atmospheric pollution characteristics
Source apportionment

ABSTRACT

Primitive electronic waste (e-waste) dismantling activities have been shown to be an important emissions source for a variety of toxic organic compounds, including carcinogenic polycyclic aromatic hydrocarbons (PAHs). Previous studies have found that some nitrated PAHs (NPAHs) are more toxic than their parent PAHs, however, little attention has been paid to the formation of PAH derivatives during e-waste processing and there is a lack of comprehensive data from field observations. In this study, the spatial distribution, temporal trends and atmospheric fate of NPAHs and hydroxylated PAHs (OH-PAHs) were investigated at typical e-waste dismantling sites, with monitoring data collected over three consecutive years. Compared to background levels, higher levels of NPAHs and OH-PAHs were found in air samples from an e-waste dismantling industrial park, with their seasonal and annual changes shown to be affected by e-waste dismantling activities. Atmospheric $PM_{2.5}$ particles were found to have high relative abundances of NPAHs (76.9%–95.1%) and OH-PAHs (73.3%–91.6%), with particle-bound concentrations ranging from 20.1 to 88.8 and 37.1 to 107 pg m^{-3}, respectively. The most abundant NPAH isomers were found to be 9-Nitroanthracene and 2-Nitrofluoranthene, while OH-PAH isomers containing 2–4 rings were predominant. Source identification was performed based on the specific diagnostic ratios of NPAH isomers, confirming that NPAH and OH-PAH emissions have multiple sources, including emissions related to the e-waste dismantling process, atmospheric photochemical reactions and traffic emissions. Further research on the fate of such derivatives and their potential use as markers for source identification, is urgently required.

1. Introduction

Primitive and intensive electronic waste (e-waste) dismantling and recycling activities, have been shown to be an important emission source for many toxic and hazardous substances, such as heavy metals (Fu et al., 2013; Wu et al., 2019), volatile organic compounds (VOCs) (An et al., 2014; Liu et al., 2017) and semi-volatile organic compounds (SVOCs) (An et al., 2011; Liu et al., 2019; Ma et al., 2022). These e-waste processing activities have resulted in high concentrations of contaminants being transferred from e-waste dismantling sites into natural environments, raising concerns about the potential exposure risk and health consequences for workers and residents in the surrounding area (Chen et al., 2011). For example, the production of relatively high concentrations of carcinogenic polycyclic aromatic hydrocarbons (PAHs) has been observed during e-waste recycling processes (Deng et al., 2006; Zhang et al., 2011; Wei et al., 2012; Chen et al., 2019; Tang et al., 2020; Ma et al., 2022). The composition profiles of PAHs have been shown to vary significantly at different e-waste dismantling sites due to the wide range of temperatures used for processing the various types of e-waste (Zhang et al., 2011; An et al., 2014). There is also

---

☆ This paper has been recommended for acceptance by Charles Wong.

* Corresponding author. Guangdong-Hong Kong-Macao Joint Laboratory for Contaminants Exposure and Health, Guangdong Key Laboratory of Environmental Catalysis and Health Risk Control, Institute of Environmental Health and Pollution Control, Guangdong University of Technology, Guangzhou, 510006, China.

E-mail address: antc99@gdut.edu.cn (T. An).

https://doi.org/10.1016/j.envpol.2022.119713
Received 8 April 2022; Received in revised form 30 June 2022; Accepted 1 July 2022
Available online 6 July 2022

concern about the possible release of PAH transformation products, as monitoring reports have indicated the occurrence of nitrated PAHs (NPAHs) bound to fine particulate matter ($PM_{2.5}$, diameter <2.5 μm) in atmospheric samples collected from an e-waste site (Wei et al., 2012). A lab-based simulation study also verified the emission of NPAHs from pyrolytic e-waste disposal processes (Huang et al., 2014a, 2014b). As reported by Simoneit et al. (2007), hydroxylated PAH derivatives (OH-PAHs) are also oxidation products of PAHs that can be emitted directly from different incomplete combustion processes. OH-PAHs have also been widely identified as urinary metabolites in e-waste dismantling workers (Ma et al., 2022), however, the study on the OH-PAHs emissions from the pyrolysis of e-waste is limited. Numerous studies have demonstrated the mutagenicity and carcinogenicity of these PAH derivatives (Durant et al., 1996; Benbrahim-Tallaa et al., 2012), with certain isomers of NPAHs and OH-PAHs exhibiting higher levels of toxicity and mutagenic potential than their parent PAHs (Durant et al., 1996; Song et al., 2020). However, limited data is available on the environmental occurrence and fate of PAH derivatives originating from e-waste recycling activities (Wei et al., 2012; Liu et al., 2020), and therefore, further research is needed to better understand their behavioral trends and dynamics in different environmental matrices.

PAH derivatives, such as NPAH and OH-PAH congeners, are mainly formed directly by incomplete combustion and the pyrolysis of fossil fuels and biomass, or indirectly from the homogenous and heterogeneous reactions of parent PAHs with gaseous oxidants, such as •OH, O_3 and NO_x (Bandowe and Meusel, 2017). The formation and composition profiles of these PAH derivatives have been determined based on combinations of several potential sources, such as incomplete combustion and the pyrolysis of fossil fuels and biomass, vehicle exhaust emissions and secondary formation via photochemical reactions (Walgraeve et al., 2010; Wei et al., 2012; Bandowe and Meusel, 2017). The atmospheric occurrence and distribution of NPAHs have widely been reported, including $PM_{2.5}$ bound NPAHs in both urban and rural ambient environments, with measured concentrations typically 2–3 orders of magnitude lower than their corresponding parent PAH (Du et al., 2018; Wei et al., 2015; Wang et al., 2017; Zhang et al., 2018). Residential wood combustion is a significant source of PAH derivatives in developing countries (Shen et al., 2012). In addition, NPAHs have also been identified in fine particles from diesel vehicle exhaust emissions (Pham et al., 2013; Garcia et al., 2014). Relatively high concentrations of NPAHs have previously been reported at an e-waste site in Southern China, suggesting both direct emission and secondary formation sources (Wei et al., 2012). However, limited data is available on the pollution characteristics of OH-PAHs in the atmosphere (Barrado et al., 2012; Lin et al., 2015; Ma et al., 2016). The sources of atmospheric OH-PAHs are not well understood, but they may be related to traffic emissions and secondary formation in warm seasons when heating sources are not widely used, or biomass burning during cold seasons when heating is required (Lin et al., 2015). Biomass burning has been reported to be the dominant source of OH-PAHs in $PM_{2.5}$ in Hong Kong (Ma et al., 2016). The occurrence of OH-PAHs has also been investigated in surface soils in Southern China, indicating that they may be derived from the breakdown of their parent PAHs in the atmosphere and/or soil (Gao et al., 2019). OH-PAHs also serve as biomarkers for human exposure to multiple classes of PAHs and have frequently been detected in human biological samples such as hair, nails and urine (Lu et al., 2016; Lin et al., 2019; Lin et al., 2020; Ma et al., 2021). High concentrations of OH-PAHs have also been reported in occupational exposure groups, such as e-waste facility workers (Lu et al., 2016; Lin et al., 2019). However, the occurrence and distribution of these metabolites in the atmospheric environment of e-waste processing sites remains unclear.

The gas-particle partitioning (Shen et al., 2012; Wei et al., 2015; Zhang et al., 2018), particle phase size distribution (Du et al., 2018) and seasonal variation (Wei et al., 2012; Bandowe et al., 2014) of PAH derivatives have also been reported. In general, a higher proportion of NPAHs tend to exist in the particulate phase than their parent PAHs, which might be related to the greater polarity, higher molecular weight and lower vapor pressure of these derivatives (Shen et al., 2012; Zhang et al., 2018). Nearly 90% of NPAHs were associated with $PM_{2.5}$ particles, and ultrafine particulate matter ($PM_{1.0}$, diameter <1.0 μm) over winter months (Du et al., 2018). However, studies have indicated that these gaseous compounds accounted for 29–44% of the total health risk in March and September from an urban site in Xi'an, central China (Wei et al., 2015). The changes in concentrations between the gaseous and particulate forms of PAH derivatives exhibit significant seasonal variations, with higher levels observed in colder winter periods than in warmer summer periods (Barrado et al., 2012; Wei et al., 2012; Bandowe et al., 2014). The spatial and seasonal variation in these pollutants is also significantly affected by meteorological conditions, such as the ambient temperature, humidity, atmospheric pressure and wind speed (Bandowe et al., 2014). However, comprehensive data is lacking for the emission, distribution and deposition of PAH derivatives from e-waste processing sites.

In the present study, the atmospheric occurrence of NPAHs and OH-PAHs were investigated in gas phase and atmospheric particulate matter ($PM_{2.5}$, PM_{10} and TSP) samples collected over three consecutive years at a typical e-waste disposal site from southern China. The spatial and temporal (including seasonal) variability of the target PAH derivatives were analyzed and correlations between the concentrations of NPAHs and OH-PAHs in atmospheric emissions from e-waste treatment were investigated over three consecutive years. In addition, the variations in these target PAH derivatives were also analyzed to determine possible sources, especially for the secondary emission of NPAHs via photochemical formation.

2. Materials and methods

2.1. Sample collection

This study was carried out at a typical e-waste dismantling site in Southern China in the April, July, November of 2015, and January of 2016 representing the four seasons, and in November of 2016 and 2017 representing autumn, respectively. A detailed description of the air sampling dates, temperature, relative humidity, wind direction and wind speed are provided in the supporting information (SI) (Table S1), as well as a map of the study area showing the location of sampling sites (Fig. 1). Briefly, air samples were collected at a typical e-waste dismantling industrial park (EP, 23°19′41″N, 116°21′43″E) and its surrounding area within a 1 km distance, including a roadside (RS, 23°21′25″N, 116°23′06″E) and a residential area (RA, 23°19′08″N, 116°20′49″E). The e-waste dismantling industrial park (EP) covers an area of 300, 000 m^2, with both the raw e-waste and valuable recycled materials being transported by heavy-duty diesel vehicles. The emission of e-waste pollutants has been shown to mainly originate from recycling waste plastics by the formation of granules, as well as the melting of tin of waste printed circuit boards using muffle furnaces for the recycling of valuable electronic components (Ma et al., 2022). The use of coal or wood burning stoves, open-air burning and acid baths to recover valuable materials from e-waste, have been banned since the EP became operational at end of 2013. A village (VS, 23°17′49″N, 116°20′55″E) 4 km away from EP site was selected as the control site, in which the resident mainly used electricity and natural gas for their daily energy supply. For comparison, a sampling site in Guangzhou (GZ, 23°08′49″N, 113°21′29″E) was selected to represent the pollution characteristics from an urban area in Southern China that is located a significant distance (400 km) from the EP site.

A detailed description of the sampling methods used have been described in a previous study (Chen et al., 2019). Briefly, particulate matter samples, including $PM_{2.5}$, PM_{10} and TSP, as well as their corresponding gaseous samples, were collected simultaneously by drawing air through quartz fiber filters (QFFs, 20.3 cm × 25.4 cm, Whatman, UK) followed by polyurethane foams (PUF) plugs, using high-volume air

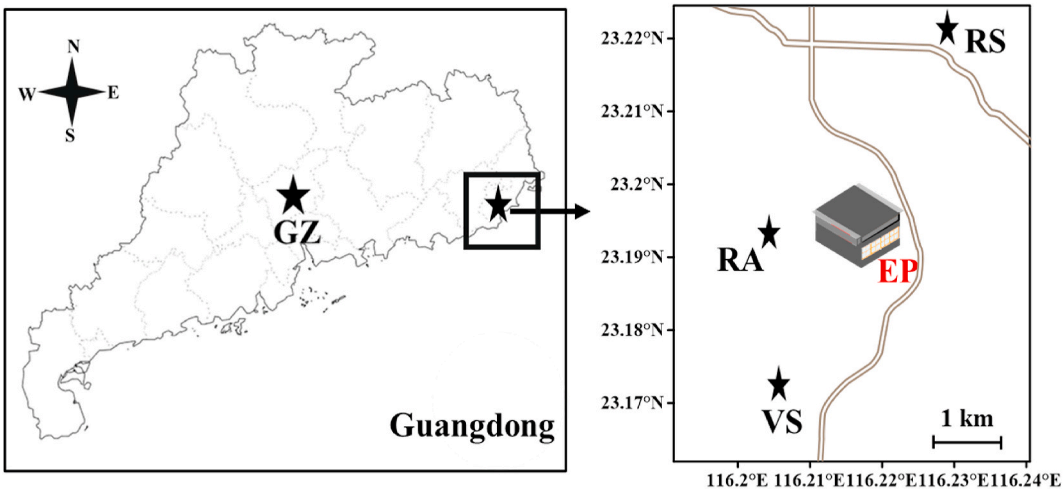

Fig. 1. Map of the study area showing location of sampling sites.

samplers (Guangzhou Mingye Instrument Plant, China), at a flow rate of 0.3 m^3 min^{-1} and a height of 1.5–2 m above the ground. The sampling time is 8 h in the daytime with three samples collecting at each sampling sites. After collection, the samples were wrapped in pre-cleaned aluminum foil, sealed in zip-locked polyethylene bags stored in the dark at −20 °C prior to analysis.

2.2. Sample extraction and instrumental analysis

Standards of nine NPAHs (9-NAnt, 3-NPhe, 2-NFluA, 3-NFluA, 1-NPyr, 2-NPyr, 7-NBaA, 6-NChr, 6-NBaP) and twelve OH-PAHs (1-OHNap, 2-OHNap, 2-OHFlu, 3-OHFlu, 9-OHFlu, 1-OHPhe, 2-OHPhe, 3-OHPhe, 4-OHPhe, 9-OHPhe, 1-OHPyr, 6-OHChr, 3-OHBaP) isomers were purchased from AccuStandard (New Haven, CT, US), Chiron AS (Trondheim, Norway), Toronto Research Chemicals (North York, ON, Canada) and Dr. Ehrenstorfer GmbH (Augsburg, Germany). Isotopically labeled standards were obtained from Cambridge Isotope Laboratories (Andover, MA, US). Additional details are provided in the SI (Table S2).

The analytical methods employed were based on those reported in previous studies (Chen et al., 2019; Liu et al., 2020), with the procedures used for the extraction, cleanup and purification of samples described in detail in the supporting information (Text S1). The analysis of NPAHs was carried out using an Agilent 7890B gas chromatography coupled with a 5977B mass spectrometer (GC-MS) in electron capture negative ionization mode. OH-PAHs were quantified using an Agilent 1260 liquid chromatography system coupled with a 6470 triple quadrupole mass spectrometer (LC-MS/MS) with electron spray ionization in multiple reaction monitoring mode. A detailed description of these procedures is provided in the SI (Text S1).

2.3. Quality assurance and quality control

A procedural blank and a spiked sample were processed for every batch of ten field samples, with the target analytes confirmed to be nondetectable in blank samples. The relative standard deviation (RSD) of target compounds in the standard spiked samples and surrogate field samples standards were <10%. The recovery of target compounds in the standard spiked samples and surrogate standards in field samples ranged from 78.2% to 122% (Table S3). Therefore, the concentration of target compounds in all field samples were not corrected according to the surrogate standards. A seven-point calibration was used to quantify each individual compound and the regression coefficients (R^2) of all calibration curves were $\geq$0.99. The limits of detection for the method (mLOD) ranged from 1.7 to 9 pg m^{-3} and from 1.7 to 83 pg m^{-3} for each NPAH and OH-PAH isomer, respectively, with mLOD values provided in Table S3.

2.4. Statistical analysis

Source apportionment of the derivatives of PAHs was carried out using principal component analysis (PCA) in combination with specific diagnostic ratios for individual isomers. The Kolmogorov-Smirnov test was used to determine a normal distribution, with groups that did not meet the normality assumption compared using a nonparametric test. The differences in target analyte concentrations between the two groups were analyzed using the Mann-Whitney *U* test, while the Pearson correlation coefficient (R) was used to determine the correlations between concentrations of NPAHs or OH-PAHs and their parent PAH. All statistical analysis was carried out using SPSS v.13.0 software, with $p < 0.05$ indicating statistically significant differences. Values below the limit of quantification for the method (mLOQ) but above the mLOD, were assigned a value of mLOQ/2.

3. Results and discussion

3.1. Spatial distribution of NPAHs and OH-PAHs in TSP, PM10 and PM2.5

As shown in Fig. 2, the concentration ranges of the total NPAHs and OH-PAHs (TSP plus gaseous phase) at the EP sites were 46.6–142 and 75.9–291 pg m^{-3}, respectively, with higher concentration of OH-PAHs than NPAHs potentially ascribed to the contribution from hydroxynaphthalene. Nevertheless, the concentrations of both NPAHs and OH-PAHs were lower than their corresponding parent PAH (25.9–88.7 ng m^{-3}) in the same samples, indicating a difference of 2–3 orders of magnitude (Chen et al., 2019). The highest concentration (TSP plus gaseous phase) of NPAHs was found at the RS site, with a median concentration of 142 pg m^{-3}, followed by EP, RA, GZ and VS sites, with median concentrations of 131, 65.6, 57.4 and 46.6 pg m^{-3}, respectively. In contrast to the spatial distribution of NPAHs, the concentrations of OH-PAHs were highest at the EP site, followed by RS, VS, RA and GZ, with median concentrations of 291, 170, 133, 92.7 and 75.9 pg m^{-3}, respectively. The concentrations of NPAHs and OH-PAHs at the EP and RS sites were significantly higher than those at typical urban site of GZ (Mann-Whitney *U* test, $p < 0.05$). Furthermore, non-significant differences were observed between NPAH and OH-PAH concentrations at the RA and GZ sites ($p > 0.05$). This indicates that at the EP site, e-waste dismantling is an important source of NPAHs and OH-PAHs, while at the RS site, traffic emissions were the main source of NPAHs and OH-PAHs, as the RS site is next to a main road outside of the e-waste disposal

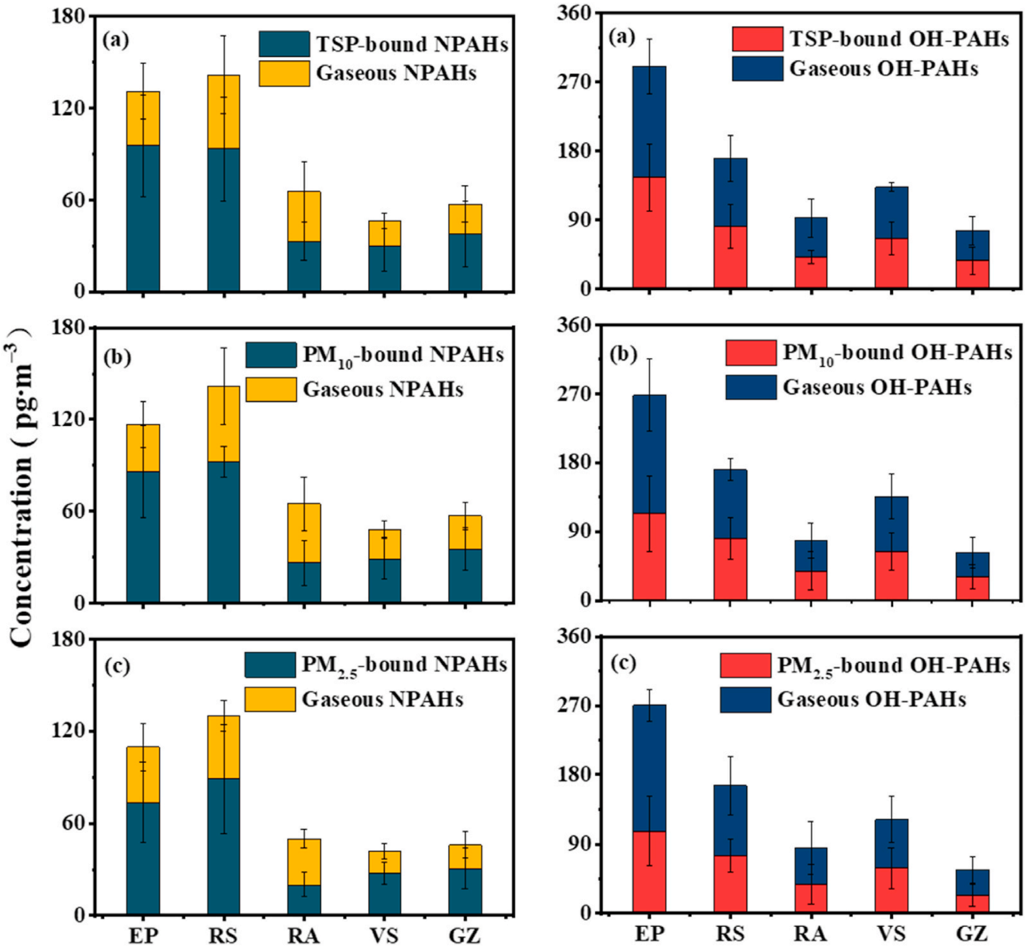

Fig. 2. Concentrations of NPAHs and OH-PAHs in particulate (TSP, PM_{10}, and $PM_{2.5}$) and in gaseous phases at different sampling sites.

industrial park.

Limited data is available on the occurrence of PAH derivatives in atmospheric samples from other EP sites. However, the concentrations of NPAHs found in the present study were slightly lower than the concentrations of $PM_{2.5}$-bound NPAHs reported at another EP site in Qingyuan (Southern China), which reported concentrations ranging from 40.9 to 645 pg m^{-3} (Wei et al., 2012). However, the concentrations of $PM_{2.5}$-bound NPAHs found at EP sites in Southern China were lower than those reported in urban air in Xi'an (Wei et al., 2015; Wang et al., 2017), rural air in Shanxi (Du et al., 2018), as well as in urban, mountainous and marine sites in Shandong (Zhang et al., 2018) (Northern China), which have been found to mainly originate from coal and biomass combustion. The concentrations of NPAHs in the present study were also lower than those reported for a rural site in the Pearl River Delta region (China) (Huang et al., 2014a, 2014b). The $PM_{2.5}$-bound concentrations of NPAHs at the EP site in the present study were similar to these nonpoint source reported for Sapporo, Kanazawa, Tokyo, Sagamihara and Kitakyushu in Japan, with NPAH concentrations ranging from 0.5 to 141 pg m^{-3} detected from 1997 to 2014 (Hayakawa et al., 2018), but were higher than those reported for Oregon (US) with concentrations <15 pg m^{-3} (Lafontaine et al., 2015). Unfortunately, no data is available for comparison of atmospheric OH-PAHs at the EP site. The concentrations of $PM_{2.5}$-bound OH-PAHs in this study were similar to those reported for an urban site in Hong Kong, with a median concentration of 31.6 pg m^{-3} (Ma et al., 2016). The results of the present study indicate that primitive e-waste disassembly is an important source of OH-PAH emissions in Southern China, although the measured concentrations are far lower than those produced by coal and biomass combustion heating in Northern China during winter periods (Wei et al., 2015; Wang et al., 2017; Du et al., 2018).

The concentrations of NPAHs in the particle phase of TSP, PM_{10} and $PM_{2.5}$ were 29.9–95.6, 26.4–92.8 and 20.1–88.8 pg m^{-3}, respectively, while the concentrations of OH-PAHs were 41.6–145, 38.9–114 and 37.1–107 pg m^{-3}, respectively (Fig. 2). These results show that a majority of detected NPAHs (76.9%–95.1%) and OH-PAHs (73.3%–91.6%) were associated with $PM_{2.5.}$ Similar distribution patterns have previously been reported for PAHs in atmospheric particulates of the same samples (Chen et al., 2019). Overall, 60.1%–73.5% of NPAHs were detected in the particulate phase at all the sampling sites except RA, which had a relatively higher proportion of NPAHs in the gaseous phase, potentially due the influence of e-waste emissions, as the spatial diffusion of NPAHs is faster in the gaseous phase. Similar results have also been reported for the atmosphere of the Pearl River Delta (PRD) in Southern China, with 76.6% of PAHs existing in the particle phase (Huang et al., 2014a, 2014b). These results indicate that a majority of atmospheric NPAHs are associated with $PM_{2.5}$. In contrast, only 39.5%–50.0% of OH-PAHs were found to exist in the particle phase, suggesting that these derivatives are more uniformly distributed between the gas phase, which may be due to hydroxynaphthalene, as the predominated compound of total OH-PAHs, easier distributed in the gas phase.

The isomers 9-NAnt and 2-NFluA were the most abundant NPAHs, accounting for 66.7%–74.4% of total NPAHs (Fig. 3). Among all NPAHs, 9-NAnt and 3-NPhe exhibited the highest concentrations in the gas phase, accounting for 81.8%–92.1% of total gaseous NPAHs (Fig. S1). In the particle phase, 9-NAnt, 2-NFluA and 2-NPyr exhibited the highest concentrations, accounting for 82.6%–89.5% of total NPAHs. Similar results have been reported at rural sampling sites in the Pearl River Delta of Southern China (Huang et al., 2014a, 2014b). Among OH-PAHs, the

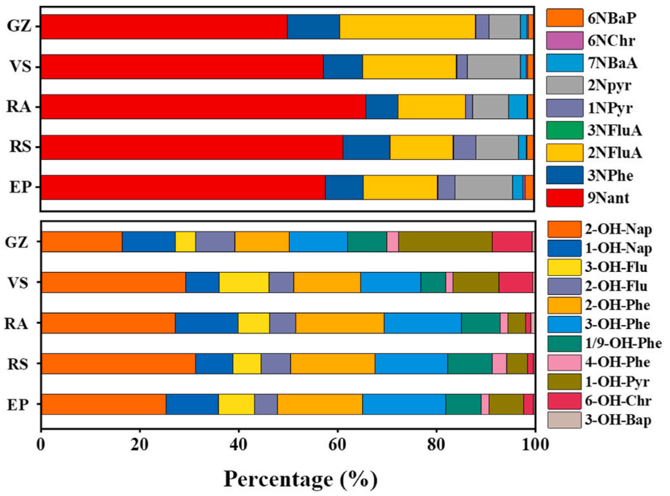

Fig. 3. Composition profiles of NPAH (a) and OH-PAHs (b) in the atmospheric samples collected at different sampling sites.

concentrations of 2-OH-Nap, 2-OH-Phe, 3-OH-Phe and 1-OH-Pyr were highest, accounting for 64.1%–67.2% of total OH-PAHs (Fig. 3). In the gas phase, the concentration of 2-OH-Nap was highest, accounting for 58.7%–69.2% of total OH-PAHs. In the particle phase, the concentrations of 2-OH-Phe, 3-OH-Phe and 1-OH-Pyr were relatively high, accounting for 65.1%–86.5% of total OH-PAHs.

In terms of gas and particle phase distribution, the 3-ring NPAHs were equally distributed in both gas and particle phases, while 4–5 ring NPAHs were mainly distributed in the particle phase. Similar results have been observed for OH-PAHs, with isomers containing 3–4 rings associated with the particle phase. Compared to their corresponding parent PAHs, NPAHs and OH-PAHs have larger molecular weights and are more polarized due to the electronic effects of substituents, resulting in a tendency to more easily adhere to particulate matter (Huang et al., 2014a, 2014b). Therefore, NPAHs and OH-PAHs with fewer than three benzene rings tend to be distributed in the gas phase, while derivatives with three or more benzene rings tend to be distributed in the particle phase, especially in fine particulate matter.

3.2. Temporal trends of NPAHs and OH-PAHs in TSP

At the EP site, air samples contained significantly higher concentrations of NPAHs (TSP plus gaseous phase) in the spring season of 2015, with a mean concentration of 236 pg m^{-3} ($n = 3$), while in summer, autumn and winter the mean concentrations were 55.5, 92.1 and 93.7 pg m^{-3}, respectively (Fig. S2). In the autumn period from 2015 to 2017, the atmospheric concentration of NPAHs at the EP site increased gradually, with mean concentrations in autumn of 2016 and 2017 of 106 and 183 pg m^{-3}, respectively. The seasonal and annual trends in atmospheric NPAH concentrations at the other four sampling sites were similar to those at the EP site (Fig. S2), indicating that NPAHs at the RA, VS and RS sites may be affected by diffusion from the EP site. In addition to the impact of primitive e-waste processing emissions, NPAH concentrations at the RS site may be affected by vehicular emissions. Similarly, NPAH concentrations at the GZ site may be related to traffic emissions, as vehicle exhaust emissions are a main source of NPAHs in urban air.

The atmospheric concentration of OH-PAHs (TSP plus gaseous phase) measured at the EP site were highest in the spring of 2015 at 470 pg m^{-3}, followed by winter, summer and autumn, with mean concentrations of 340, 172 and 155 pg m^{-3}, respectively (Fig. S2). The atmospheric concentration of OH-PAHs in the autumn of 2016 was higher at the EP site (498 pg m^{-3}) than in the autumn of 2015 (155 pg m^{-3}), then decreased by 235 pg m^{-3} in the autumn of 2017. The seasonal and annual changes in OH-PAH concentrations at the EP site were similar to those previously reported for PAHs (Chen et al., 2019) and might be affected by the primitive e-waste recycling activities. As shown in Fig. S2, the annual trend of variation in atmospheric OH-PAH concentrations at the other four sampling sites were similar to the trend observed at the EP site. In particular, the seasonal variations of OH-PAH at the RA and RS sites were most similar to the EP site, with concentrations ranging from 59.1 to 111 pg m^{-3} and 96.6–142 pg m^{-3}, respectively, ranked in descending order from spring > winter > autumn > summer. Similar to NPAHs, higher concentrations of OH-PAHs in spring at the RS site may be derived from traffic emissions in addition to e-waste sources. Further, the relative humidity (78–86%) in spring at the time of sampling is higher than that in other seasons, while the wind speed (6–8 km/h) is lower than that in other seasons, which could affect the diffusion of pollutants, resulting in higher concentrations of NPAHs and OH-PAHs observed. The OH-PAH concentrations at the VS site ranged from 96.6 to 142 pg m^{-3} and were ranked in descending order from spring > summer > autumn > winter. The level of atmospheric pollution observed at the GZ site was similar to the VS site, with OH-PAH concentrations decreasing from spring to winter, ranging from 31.8 to 107 pg m^{-3}, which might due to the influence of anthropogenic activities.

3.3. NPAH and OH-PAH source identification

Since the atmospheric concentrations of FluA and Pyr were comparable (Chen et al., 2019) in the same samples, the ratio of 2-NFluA to 1-NPyr and 2-NPyr can be used to determine whether NPAHs mainly originate from combustion sources or photochemical transformation (Arey et al., 1986; Atkinson et al., 1990; Bandowe and Meusel, 2017). As shown in Fig. 4, most of the 2-NFluA/1-NPyr ratios measured at the EP site were below 5 (except in autumn), indicating that the formation of NPAHs at the EP site mainly originated from combustion sources. The ratios of 2-NFluA/2-NPyr at the EP site were all close to 10, indicating that the formation of NPAHs occurred mainly through the reaction with ·OH radicals. The distribution of 2-NFluA/1-NPyr and 2-NFluA/2-NPyr ratios at the RS and RA sites was similar to the EP site, indicating that these areas were affected by similar sources. However, the 2-NFluA/2-NPyr ratio distribution at RA site was different from other sites, especially in autumn and winter seasons. This might be derived from relatively

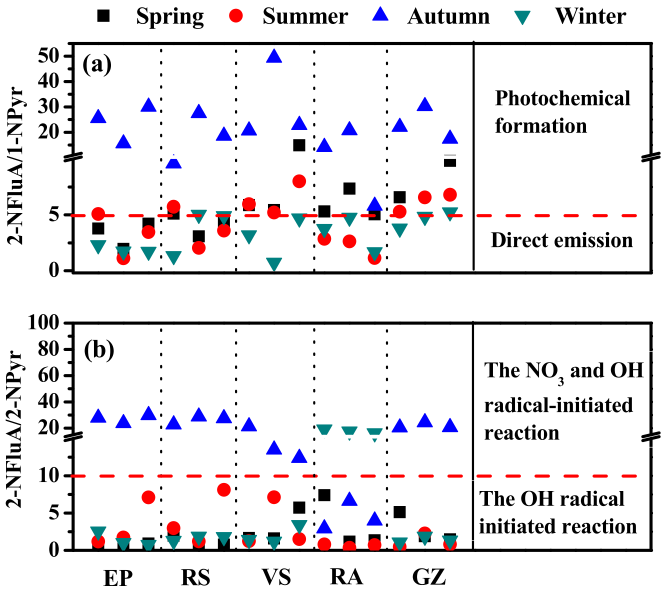

Fig. 4. The concentration ratios of 2-NFluA/1-NPyr (a) and 2-NFluA/2-NPyr (b) at different sampling sites.

lower concentrations of target NPAHs found in RA site. In addition, the variation pattern with deviation from the average value might also result in the different ratio distribution. In contrast, the 2-NFluA/1-NPyr ratio distribution at the VS and GZ sites was different from the EP site, indicating NPAHs emitted at VS and GZ originated mainly from secondary emissions, *via* the ·OH radical pathway. The EP site was located within the e-waste dismantling industrial zone, with primitive e-waste dismantling activities, such as the heating of circuit boards and motor vehicle transportation of e-waste materials, potentially being the major source of NPAHs. As the RA site was in a road side location next to the EP park, NPAH concentrations may be affected by e-waste emissions and dispersion, as well as local traffic sources. The VS and GZ sites were located in rural and urban residential areas, respectively, with the formation of NPAHs at these sites dominated by secondary sources rather than by direct combustion source emissions.

The source of atmospheric NPAHs in the study area was further analyzed by principal component analysis (PCA). At the EP site three principal components (PC1, PC2, PC3) were identified, accounting for 80.1% of the total variance (Table S4). PC1 explained 47.1% of the total variance, mainly consisting of 9-NAnt, 3-NPhe and 3-NFluA. Studies have shown that 3-NPhe is produced from incomplete coal combustion, while 9-NAnt and 3-NFluA are established markers of biomass combustion (Lin et al., 2015; Bandowe and Meusel, 2017). It has previously been reported that PAH fingerprints derived from primitive e-waste dismantling activities are similar to those from coal and biomass combustion sources, mainly due to the fact that plastic e-waste components are also composed of petrochemical products (Chen et al., 2019). Therefore, PC1 was attributed mainly to e-waste disassembly processing emissions. PC2 explained 21.6% of the total variance, mainly consisting of 2-NFluA, which is an established marker of PAH photochemical reactions (Arey et al., 1989; Atkinson et al., 1990). PC3 explained 11.4% of the total variance and may originate from traffic emissions as it consisted mainly of 6-NChr, which is consistent with the previously reported vehicle emission characteristics of 6-NChr (Alves et al., 2016). For the RS, VS, and GZ sites, three principal component factors were also identified, with the RA site found to be influenced by two distinct principal component factors. Similar to the EP site, NPAHs are found to mainly derive from primitive e-waste disassembly processes (PC1) at sites within short-range of the e-waste dismantling (RS, VS and RA). In contrast, at the GZ site, NPAHs were found to mainly originate from traffic emissions (PC1), while photochemical reactions (PC2) and coal and biomass burning (PC3) contributed relatively little to atmospheric NPAH levels at GZ.

A multivariate linear regression method (full detail is given in Text S2) was also used to calculate the contribution of each principal component factor to the total concentration of NPAHs at each sampling site. As shown in Fig. 5, at the EP site, the contributions of factor 1 (e-waste disassembly process), factor 2 (photochemical reaction) and factor 3 (traffic emissions) to the total concentration of NPAHs were 78.2%, 20.3% and 1.5%, respectively. At the VS site, the contributions of factor 1, factor 2 and factor 3 to the total concentration of NPAHs were 38.7%, 49.6% and 11.7%, respectively, while at the RA site, the contributions of factors 1 and 2 to total NPAH concentrations were 56.1% and 43.9%, respectively. This indicates that the EP site was affected by a combination of atmospheric pollutant diffusion, photochemical reactions and other local pollution sources. NPAHs at the RA and VS sites also originated from emissions and diffusion from the processing of e-waste as these sites were located in the area close to the EP site, where e-waste disassembly takes place. The results for the RS site were similar to those for the GZ site, with the contributions of factors 1, 2 and 3 being 36.0%, 12.6% and 51.4%, respectively at the RS site and 15.1%, 26.4% and 58.6% at the GZ site. Although NPAHs at the RS site were also affected by the processing of e-waste, traffic emissions were found to be the major source. NPAHs at the GZ site were also found to originate mainly from traffic emissions and atmospheric photochemical reactions. These PCA results were generally consistent with the results obtained from the specific NPAH diagnostic ratios used to discriminate between emission sources. Both methods show that NPAH emissions from e-waste dismantling activities in a typical e-waste site are commonly mixed with other sources, such as photochemical reactions and traffic emissions. Due to the lack of information on OH-PAH markers emitted from different pollution sources and the corresponding special diagnostic ratios, the sources of OH-PAHs were not analyzed in this study.

3.4. Correlation analysis for NPAHs with PAHs and OH-PAHs

Among all target NPAHs and OH-PAHs, only the concentrations of 1-NPyr exhibited significant differences between sampling sites with different sources (Mann-Whitney *U* test, $p = 0.034$). In particular, for sampling sites where NPAHs were derived from primary sources, the concentrations of 1-NPyr were significantly higher than at sites with NPAHs originating from both primary and secondary sources, which was consistent with a previous report finding that 1-NPyr mainly originated from primary emissions (Shen et al., 2012). To further analyze the correlations between Pyr, 1-NPyr and 1-OHPyr, previously reported PAH data was also considered (Chen et al., 2019), as shown in Fig. 6. Results indicated that 1-NPyr was moderately correlated with Pyr ($p = 0.041$, $R = 0.483$), while being strongly correlated with 1-OHPyr ($p =$

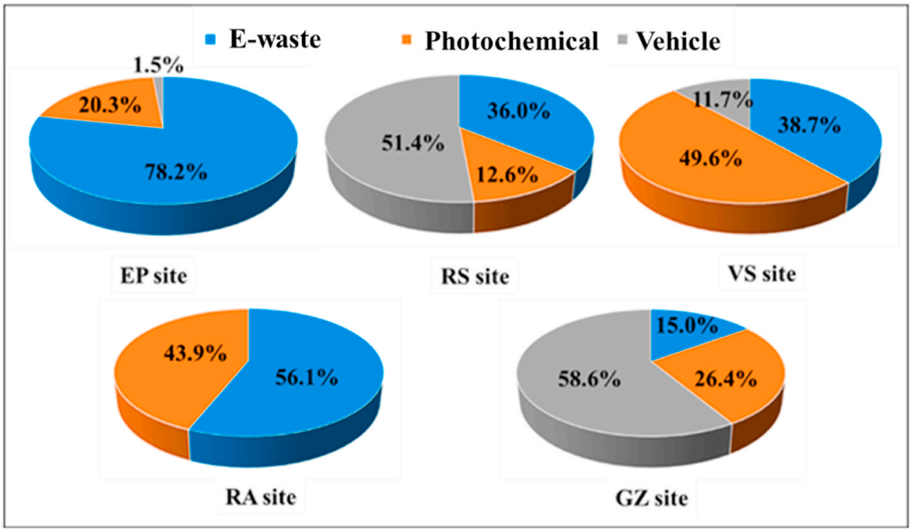

Fig. 5. Source contributions (%) of NPAHs at different sampling sites.

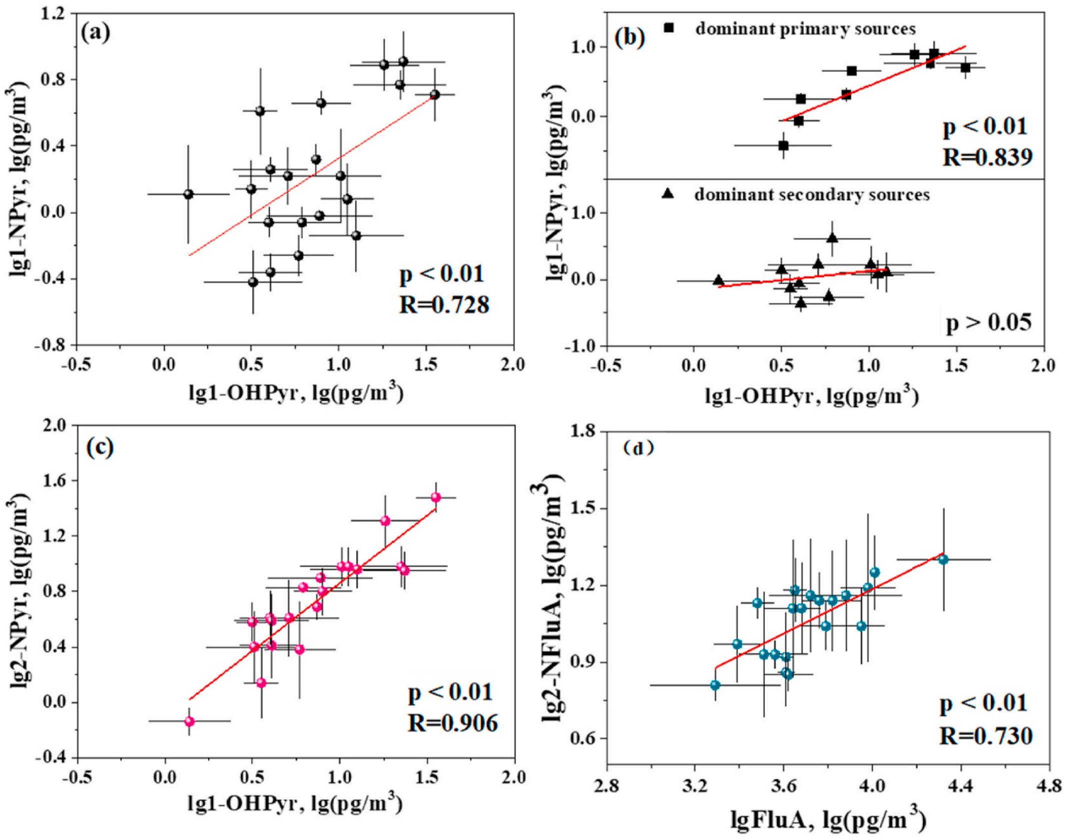

Fig. 6. Correlations between 1-OHPyr and 1-NPyr (a: total; b: predominantly primary or secondary sources, respectively), 1-OHPyr and 2-NPyr (c), and 2-NFluA and FluA (d) at the e-waste dismantling area.

0.000, R = 0.728). At sampling sites where primary emissions were the main source, 1-NPyr was strongly correlated with 1-OHPyr ($p = 0.005$, R = 0.839), while at sampling sites where secondary sources dominated, these two derivatives showed little correlation ($p > 0.05$). This may be due to 1-OHPyr being produced from primary emission sources, such as incomplete combustion (Simoneit et al., 2007; Avagyan et al., 2016), as well as from photochemical reactions (Miet et al., 2009). 1-NPyr mainly originates from primary emission sources, while photochemical reactions contribute very little (Zimmermann et al., 2012). In addition, 1-OHPyr can be photochemically produced from 1-NPyr (van den Braken-van Leersum et al., 1987), which would influence the correlation between these derivatives when secondary emission sources were dominant. Therefore, in the e-waste dismantling area examined in the present study, significant linear relationships were observed between 1-NPyr and 1-OHPyr at sampling sites affected by primary emission sources, while no correlation was found at sites affected by secondary sources.

In addition, analysis of 2-NPyr correlations with Pyr and 1-OHPyr showed that 2-NPyr was moderately correlated with Pyr ($p = 0.007$, R = 0.572) and strongly correlated with 1-OHPyr ($p = 0.000$, R = 0.906), irrespective of whether the NPAHs were derived from primary or secondary emission sources. This is consistent with previously reported results from a simulation chamber study, showing that 2-NPyr was mainly generated through the gas phase reaction of 1-OHPyr, and the reaction mechanism involved in the initially formation of OH adduct of pyrene as intermediate (Arey et al., 1989; Atkinson et al., 1990). Similarly to 2-NPyr, 2-NFluA was also found to be significantly linearly correlated with FluA ($p = 0.000$, R = 0.730) (Fig. 6). 2-NFluA and FluA were shown to be strongly correlated ($p < 0.01$) irrespective of whether their sources were primary or secondary, which may be because 2-NFluA is mainly produced by gas phase photochemical reactions (Arey et al., 1989; Atkinson et al., 1990).

Other target NPAHs observed in this study included 9-NAnt, 3-NPhe, 7-NBaA, 6-NChr and 6-NBaP, which can be produced from either primary (Shen et al., 2012; Shen et al., 2013; Alves et al., 2016; Vicente et al., 2016) or secondary sources (Jariyasopit et al., 2014a, 2014b; Cochran et al., 2016). A strong level of correlation was observed between 9-NAnt and Ant ($p = 0.001$, R = 0.669), as shown in Fig. 7. At sampling sites where primary emission sources dominated, 9-NAnt continued to be strongly correlated with Ant ($p = 0.012$, R = 0.789), while this correlation became weaker at sampling sites where secondary sources dominated ($p = 0.049$, R = 0.598). This indicates that 9-NAnt is produced more by primary emission sources in the atmospheric environment, which is consistent with the previous results of Lin et al. (2015).

Correlation analysis between 3-NPhe and Phe, 2-OHPhe, 3-OHPhe, 4-OHPhe and 1-OHPhe/9-OHPhe, showed that 3-NPhe was strongly correlated with Phe ($p = 0.000$, R = 0.708) and moderately correlated with 2-OHPhe, 3-OHPhe, 4-OHPhe and 1-OHPhe/9-OHPhe ($p < 0.05$, R = 0.422–0.527) (Fig. 7 and S3). For the sampling sites where primary emission sources were dominant, 3-NPhe was also found to be significantly correlated with Phe and OHPhe ($p < 0.05$, R = 0.425–0.705), indicating that 3-NPhe, 2-OHPhe, 3-OHPhe, 4-OHPhe and 1-OHPhe/9-OHPhe could be generated by the same primary emission sources, which is consistent with the reports of Shen et al. (2012) and Avagyan et al. (2016). At the sampling site where secondary sources were dominant, the degree of linear correlation between 3-NPhe and Phe was stronger than at sampling sites where primary sources were dominant ($p = 0.011$, R = 0.730), indicating that atmospheric 3-NPhe was mainly derived from photochemical reactions. These results were similar to the findings of Lin et al. (2015). However, correlation analysis indicated that 3-NPhe was independent of the four OHPhe isomers, which may be due to the formation of 3-NPhe from nighttime reaction of Phe with $\cdot NO_3$ radicals, rather than from the ·OH radical reaction initiated during

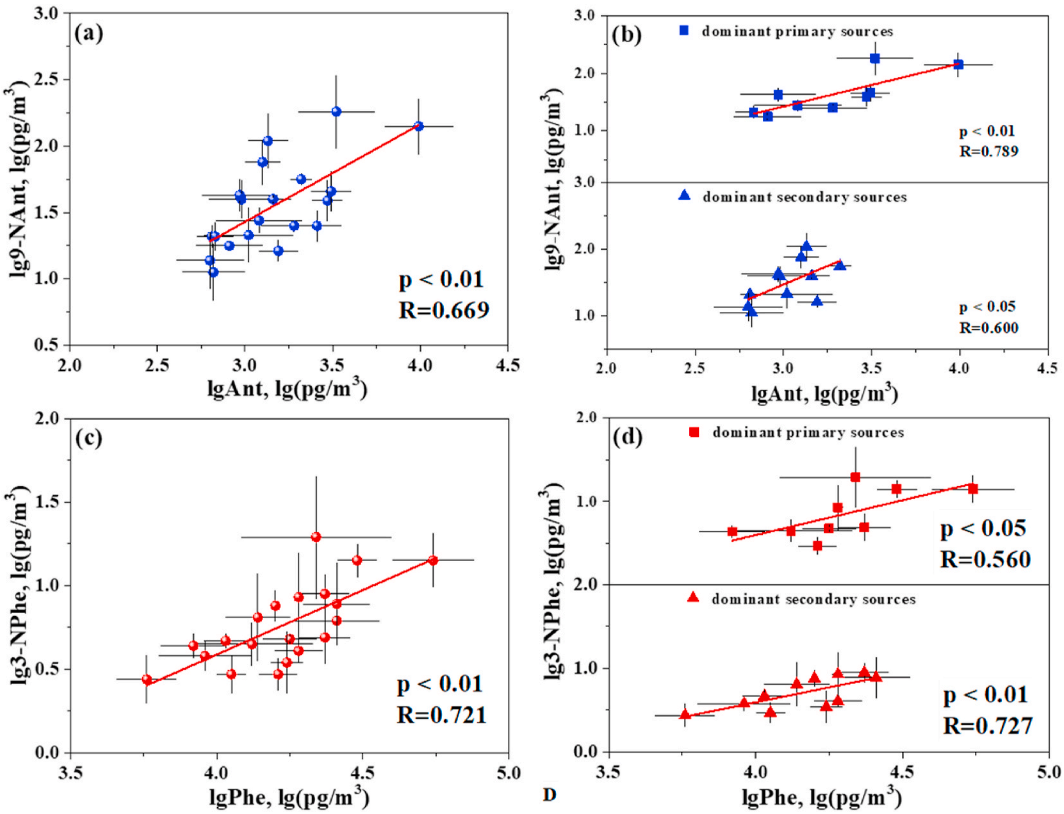

Fig. 7. Correlations between 9-NAnt and Ant, 3-NPhe and Phe (a or c: total; b or d: predominantly primary or secondary sources, respectively) at the e-waste dismantling area.

daytime (Arey et al., 1989; Jariyasopit et al., 2014a, 2014b).

A significant correlation was also observed between 7-NBaA and BaA, 6-NChr and Chr, 6-NBaP and BaP ($p < 0.05$) (Table 1), although the degree of correlation was relatively weak compared to isomers with fewer benzene rings (R = 0.500–0.543). This may be due to the fact that BaA, Chr and BaP were mainly distributed in the particle phase, with heterogeneous photochemical reactions producing less nitrated derivatives (Zimmermann et al., 2013; Jariyasopit et al., 2014a, 2014b). In addition, 7-NBaA, 6-NChr and 6-NBaP can also be produced by different primary sources, such as traffic emissions, biomass combustion and coal combustion (Yang et al., 2010; Huang et al., 2014a, 2014b; Bandowe and Meusel, 2017). The mixture of emissions sources may lead to a relatively weaker level of correlation between these high molecular weight PAHs and their nitrated derivatives.

Table 1
Correlation coefficient and p values of observed lg NPAHs, lg PAHs and lg OH-PAHs.

	Source	lg 7-NBaA	lg 6-NChr	lg 6-NBaP
lg BaA		0.500*		
	1	0.521*		
	2	0.423*		
lg Chr			0.516*	
	1		0.476*	
	2		0.531*	
lg BaP				0.543*
	1			0.513*
	2			0.521*
lg 6-OHChr			–	
	1		–	
	2		–	
lg 3-OHBaP				–
	1			–
	2			–

In summary, atmospheric emissions in e-waste dismantling areas contained NPAHs, such as 2-NFluA and 2-NPyr, which are mainly produced by secondary photochemical reactions with ·OH radicals, but were associated with corresponding PAHs and OH-PAHs, at sampling sites dominated by either primary or secondary sources. Although emissions from combustion were the main source identified at sampling sites dominated by primary emission sources, atmospheric photochemical reactions still existed. For NPAHs mainly produced from direct discharge into the atmosphere, their occurrence was positively correlated to the level of corresponding parent PAH present. For NPAHs contributing to both primary and secondary sources, a significant correlation with the corresponding parent PAH was obtained.

4. Conclusions

This study includes comprehensive analysis of the atmospheric occurrence, distribution and seasonal variations (and annual variations) in NPAHs and OH-PAHs from a typical e-waste dismantling site. Significantly higher concentrations of NPAHs and OH-PAHs were found in air samples collected near the e-waste dismantling site, indicating that primitive e-waste dismantling activities were the major source of these pollutants. The concentrations of NPAHs and OH-PAHs were slightly higher in spring and winter than in summer and autumn. The target atmospheric NPAHs mainly existed in the particulate phase, while the target OH-PAHs were almost equally distributed between the gaseous and particulate phases. In addition, more than 73.3% of all particle-bound PAH derivatives were associated with $PM_{2.5}$. The application of specific diagnostic ratios in combination with principal component analysis, identified the three major emission sources of NPAHs as e-waste dismantling and processing, atmospheric photochemical reactions and traffic emissions. In addition, some isomers of NPAHs, which are mainly produced by atmospheric photochemical reactions, exhibited significant correlations with their corresponding PAHs and OH-PAHs, allowing their successful used for source apportionment analysis. For the OH-PAHs, this study was the first to investigate their atmospheric occurrence and fate in e-waste dismantling sites and the surrounding areas. Results showed that OH-PAHs may originate from a primary emission source or be generated from atmospheric photochemical reaction products or intermediates. However, comprehensive research is needed to clarify the potential application of OH-PAHs as source identification markers.

Author statement

Shengtao Ma: Methodology, Formal analysis, Writing-original draft. **Haojia Chen:** Methodology, Formal analysis. **Congcong Yue:** Data curation. **Ranran Liu:** Methodology. **Jian Tang:** Methodology, Data curation. **Meiqing Lin:** Methodology, Formal analysis. **Guiying Li:** Writing- Reviewing and Editing. **Yan Yang:** Visualization, Investigation. **Yingxin Yu:** Visualization, Investigation. **Taicheng An:** Conceptualization, Supervision.

Declaration of competing interest

The authors declare that they have no known competing financial interests or personal relationships that could have appeared to influence the work reported in this paper.

Data availability

No data was used for the research described in the article.

Acknowledgments

This work was supported by the National Natural Science Foundation of China (41731279, 41977303 and 42177409), National Key Research and Development Program (2019YFC1804503), The Chemistry and Chemical Engineering Guangdong Laboratory (1922009), the Local Innovative and Research Team Project of Guangdong Pearl River Talents Program (2017BT01Z032), and the Natural Science Foundation of Guangdong Province (2021A1515010020).

Appendix A. Supplementary data

Supplementary data to this article can be found online at https://doi.org/10.1016/j.envpol.2022.119713.

References

Alves, C.A., Vicente, A.M.P., Gomes, J., Nunes, T., Duarte, M., Bandowe, B.A.M., 2016. Polycyclic aromatic hydrocarbons (PAHs) and their derivatives (oxygenated-PAHs, nitrated-PAHs and azaarenes) in size-fractionated particles emitted in an urban road tunnel. Atmos. Res. 180, 128–137.

An, T., Huang, Y., Li, G., He, Z., Chen, J., Zhang, C., 2014. Pollution profiles and health risk assessment of VOCs emitted during e-waste dismantling processes associated with different dismantling methods. Environ. Int. 73, 186–194.

An, T., Zhang, D., Li, G., Mai, B., Fu, J., 2011. On-site and off-site atmospheric PBDEs in an electronic dismantling workshop in south China: gas-particle partitioning and human exposure assessment. Environ. Pollut. 159, 3529–3535.

Arey, J., Zielinska, B., Atkinson, R., Winer, A.M., Ramdahl, T., Pitts, J.N., 1986. The formation of nitro-PAH from the gas-phase reactions of fluoranthene and pyrene with the OH radical in the presence of NOx. Atmos. Environ. 20, 2339–2345.

Arey, J., Zielinska, B., Atkinson, R., Aschmann, S.M., 1989. Nitroarene products from the gas-phase reactions of volatile polycyclic aromatic hydrocarbons with the OH radical and N_2O_5. Int. J. Chem. Kinet. 21, 775–799.

Atkinson, R., Arey, J., Zielinska, B., Aschmann, S.M., 1990. Kinetics and nitro-products of the gas-phase OH and NO_3 radical-initiated reactions of naphthalene-d8, Fluoranthene-d10, and pyrene. Int. J. Chem. Kinet. 22, 999–1014.

Avagyan, R., Nyström, R., Lindgren, R., Boman, C., Westerholm, R., 2016. Particulate hydroxy-PAH emissions from a residential wood log stove using different fuels and burning conditions. Atmos. Environ. 140, 1–9.

Bandowe, B.A.M., Meusel, H., 2017. Nitrated polycyclic aromatic hydrocarbons (nitro-PAHs) in the environment - a review. Sci. Total Environ. 581, 237–257.

Bandowe, B.A.M., Meusel, H., Huang, R.j., Ho, K., Cao, J., Hoffmann, T., Wilcke, W., 2014. $PM_{2.5}$-bound oxygenated PAHs, nitro-PAHs and parent-PAHs from the atmosphere of a Chinese megacity: seasonal variation, sources and cancer risk assessment. Sci. Total Environ. 473–474, 77–87.

Barrado, A.I., García, S., Barrado, E., Pérez, R.M., 2012. $PM_{2.5}$-bound PAHs and hydroxy-PAHs in atmospheric aerosol samples: correlations with season and with physical and chemical factors. Atmos. Environ. 49, 224–232.

Benbrahim-Tallaa, L., Baan, R.A., Grosse, Y., Lauby-Secretan, B., El Ghissassi, F., Bouvard, V., Guha, N., Loomis, D., Straif, K., 2012. Carcinogenicity of diesel-engine and gasoline-engine exhausts and some nitroarenes. Lancet Oncol. 13, 663–664.

Chen, A., Dietrich, K.N., Huo, X., Ho, S.M., 2011. Developmental neurotoxicants in e-waste: an emerging health concern. Environ. Health Perspect. 119, 431–438.

Chen, H., Ma, S., Yu, Y., Liu, R., Li, G., Huang, H., An, T., 2019. Seasonal profiles of atmospheric PAHs in an e-waste dismantling area and their associated health risk considering bioaccessible PAHs in the human lung. Sci. Total Environ. 683, 371–379.

Cochran, R.E., Jeong, H., Haddadi, S., Derseh, R.F., Gowan, A., Beranek, J., Kubatova, A., 2016. Identification of products formed during the heterogeneous nitration and ozonation of polycyclic aromatic hydrocarbons. Atmos. Environ. 128, 92–103.

Deng, W.J., Louie, P.K.K., Liu, W.K., Bi, X.H., Fu, J.M., Wong, M.H., 2006. Atmospheric levels and cytotoxicity of PAHs and heavy metals in TSP and $PM_{2.5}$ at an electronic waste recycling site in southeast China. Atmos. Environ. 40, 6945–6955.

Du, W., Chen, Y.C., Shen, G.F., Wang, W., Zhuo, S.J., Huang, Y., Pan, X.L., Tao, S., 2018. Winter air pollution by and inhalation exposure to nitrated and oxygenated PAHs in rural Shanxi, north China. Atmos. Environ. 187, 210–217.

Durant, J.L., Busby, W.F., Lafleur, A.L., Penman, B.W., Crespi, C.L., 1996. Human cell mutagenicity of oxygenated, nitrated and unsubstituted polycyclic aromatic hydrocarbons associated with urban aerosols. Mutat. Res., Genet. Toxicol. Environ. Mutagen. 371, 123–157.

Fu, J., Zhang, A., Wang, T., Qu, G., Shao, J., Yuan, B., Wang, Y., Jiang, G., 2013. Influence of e-waste dismantling and its regulations: temporal trend, spatial distribution of heavy metals in rice grains, and its potential health risk. Environ. Sci. Technol. 47, 7437–7445.

Gao, C.J., Xia, L.L., Wu, C.C., Shen, H.M., Guo, Y., 2019. Hydroxylated polycyclic aromatic hydrocarbons in surface soil in an emerging urban conurbation in South China. Sci. Total Environ. 692, 1250–1256.

Garcia, K.O., Teixeira, E.C., Agudelo-Castaneda, D.M., Braga, M., Alabarse, P.G., Wiegand, F., Kautzmann, R.M., Silva, L.F.O., 2014. Assessment of nitro-polycyclic aromatic hydrocarbons in PM1 near an area of heavy-duty traffic. Sci. Total Environ. 479, 57–65.

Hayakawa, K., Tang, N., Nagato, E.G., Toriba, A., Sakai, S., Kano, F., Goto, S., Endo, O., Arashidani, K.I., Kakimoto, H., 2018. Long term trends in atmospheric concentrations of polycyclic aromatic hydrocarbons and nitropolycyclic aromatic hydrocarbons: a study of Japanese cities from 1997 to 2014. Environ. Pollut. 233, 474–482.

Huang, B., Liu, M., Bi, X., Chaemfa, C., Ren, Z., Wang, X., Sheng, G., Fu, J., 2014a. Phase distribution, sources and risk assessment of PAHs, NPAHs and OPAHs in a rural site of Pearl River Delta region, China. Atmos. Pollut. Res. 5, 210–218.

Huang, W., Huang, B., Bi, X.H., Lin, Q.H., Liu, M., Ren, Z.F., Zhang, G.H., Wang, X.M., Sheng, G.Y., Fu, J.M., 2014b. Emission of PAHs, NPAHs and OPAHs from residential honeycomb coal briquette combustion. Energy Fuels 28, 636–642.

Jariyasopit, N., McIntosh, M., Zimmermann, K., Arey, J., Atkinson, R., Cheong, P.H.Y., Carter, R.G., Yu, T.W., Dashwood, R.H., Simonich, S.L.M., 2014a. Novel nitro-PAH formation from heterogeneous reactions of PAHs with NO2, NO3/N2O5, and OH radica$_{l}$s: p$_{r}$ed$_{i}$c$_{t}$ion, laboratory studies, and mutagenicity. Environ. Sci. Technol. 48, 412–419.

Jariyasopit, N., Zimmermann, K., Schrlau, J., Arey, J., Atkinson, R., Yu, T.W., Dashwood, R.H., Tao, S., Simonich, S.L.M., 2014b. Heterogeneous reactions of particulate matter-bound PAHs and NPAHs with NO_3/N_2O_5, OH radicals, and O_3 under simulated long-range atmospheric transport conditions: reactivity and mutagenicity. Environ. Sci. Technol. 48, 10155–10164.

Lafontaine, S., Schrlau, J., Butler, J., Jia, Y.L., Harper, B., Harris, S., Bramer, L.M., Waters, K.M., Harding, A., Simonich, S.L.M., 2015. Relative influence of trans-Pacific and regional atmospheric transport of PAHs in the Pacific Northwest, US. Environ. Sci. Technol. 49, 13807–13816.

Lin, M., Tang, J., Ma, S., Yu, Y., Li, G., Fan, R., Mai, B., An, T., 2020. Insights into biomonitoring of human exposure to polycyclic aromatic hydrocarbons with hair analysis: a case study in e-waste recycling area. Environ. Int. 136, 105432.

Lin, M., Tang, J., Ma, S., Yu, Y., Li, G., Mai, B., Fan, R., An, T., 2019. Simultaneous determination of polybrominated diphenyl ethers, polycyclic aromatic hydrocarbons and their hydroxylated metabolites in human hair: a potential methodology to distinguish external from internal exposure. Analyst 144, 7227–7235.

Lin, Y., Ma, Y.Q., Qiu, X.H., Li, R., Fang, Y.H., Wang, J.X., Zhu, Y.F., Hu, D., 2015. Sources, transformation, and health implications of PAHs and their nitrated, hydroxylated, and oxygenated derivatives in $PM_{2.5}$ in Beijing. J. Geophys. Res. Atmos. 120, 7219–7228.

Liu, R., Chen, J., Li, G., An, T., 2017. Using an integrated decontamination technique to remove VOCs and attenuate health risks from an e-waste dismantling workshop. Chem. Eng. J. 318, 57–63.

Liu, R., Ma, S., Li, G., Yu, Y., An, T., 2019. Comparing pollution patterns and human exposure to atmospheric PBDEs and PCBs emitted from different e-waste dismantling processes. J. Hazard. Mater. 369, 142–149.

Liu, R., Ma, S., Yu, Y., Li, G., Yu, Y., An, T., 2020. Field study of PAHs with their derivatives emitted from e-waste dismantling processes and their comprehensive human exposure implications. Environ. Int. 144, 106059.

Lu, S.Y., Li, Y.X., Zhang, J.Q., Zhang, T., Liu, G.H., Huang, M.Z., Li, X., Ruan, J.J., Kannan, K., Qiu, R.L., 2016. Associations between polycyclic aromatic hydrocarbon (PAH) exposure and oxidative stress in people living near e-waste recycling facilities in China. Environ. Int. 94, 161–169.

Ma, S., Zeng, Z., Lin, M., Tang, J., Yang, Y., Yu, Y., Li, G., An, T., 2021. PAHs and their hydroxylated metabolites in the human fingernails from e-waste dismantlers: implications for human non-invasive biomonitoring and exposure. Environ. Pollut. 283, 117059.

Ma, S., Lin, M., Tang, J., Liu, R., Yang, Y., Yu, Y., Li, G., An, T., 2022. Occurrence and fate of polycyclic aromatic hydrocarbons from electronic waste dismantling activities: a critical review from environmental pollution to human health. J. Hazard. Mater. 127683.

Ma, Y., Cheng, Y., Qiu, X., Lin, Y., Cao, J., Hu, D., 2016. A quantitative assessment of source contributions to fine particulate matter ($PM_{2.5}$)-bound polycyclic aromatic hydrocarbons (PAHs) and their nitrated and hydroxylated derivatives in Hong Kong. Environ. Pollut. 219, 742–749.

Miet, K., Le Menach, K., Flaud, P.M., Budzinski, H., Villenave, E., 2009. Heterogeneous reactions of ozone with pyrene, 1-hydroxypyrene and 1-nitropyrene adsorbed on particles. Atmos. Environ. 43, 3699–3707.

Pham, C.T., Kameda, T., Toriba, A., Hayakawa, K., 2013. Polycyclic aromatic hydrocarbons and nitropolycyclic aromatic hydrocarbons in particulates emitted by motorcycles. Environ. Pollut. 183, 175–183.

Shen, G.F., Tao, S., Wei, S.Y., Chen, Y.C., Zhang, Y.Y., Shen, H.Z., Huang, Y., Zhu, D., Yuan, C.Y., Wang, H.C., Wang, Y.F., Pei, L.J., Liao, Y.L., Duan, Y.H., Wang, B., Wang, R., Lv, Y., Li, W., Wang, X.L., Zheng, X.Y., 2013. Field measurement of emission factors of PM, EC, OC, parent, nitro-, and oxy- polycyclic aromatic hydrocarbons for residential briquette, coal cake, and wood in rural Shanxi, China. Environ. Sci. Technol. 47, 2998–3005.

Shen, G.F., Tao, S., Wei, S.Y., Zhang, Y.Y., Wang, R., Wang, B., Li, W., Shen, H.Z., Huang, Y., Chen, Y.C., Chen, H., Yang, Y.F., Wang, W., Wang, X.L., Liu, W.X., Simonich, S.L.M., 2012. Emissions of parent, nitro, and oxygenated polycyclic aromatic hydrocarbons from residential wood combustion in rural China. Environ. Sci. Technol. 46, 8123–8130.

Simoneit, B.R.T., Bi, X., Oros, D.R., Medeiros, P.M., Sheng, G., Fu, J., 2007. Phenols and hydroxy-PAHs (arylphenols) as tracers for coal smoke particulate matter: source tests and ambient aerosol assessments. Environ. Sci. Technol. 41, 7294–7302.

Song, Y., Zhang, Y., Li, R., Chen, W., Chung, C.K.A., Cai, Z., 2020. The cellular effects of $PM_{2.5}$ collected in Chinese Taiyuan and Guangzhou and their associations with polycyclic aromatic hydrocarbons (PAHs), nitro-PAHs and hydroxy-PAHs. Ecotoxicol. Environ. Saf. 191, 110225.

Tang, J., Ma, S., Liu, R., Yue, C., Li, G., Yu, Y., Yang, Y., An, T., 2020. The pollution profiles and human exposure risks of chlorinated and brominated PAHs in indoor dusts from e-waste dismantling workshops: comparison of GC-MS, GC-MS/MS and GC×GC-MS/MS determination methods. J. Hazard. Mater. 394, 122573.

van den Braken-van Leersum, A.M., Tintel, C., Vantzelfde, M., Cornelisse, J., Lugtenburg, J., 1987. Spectroscopic and photochemical properties of mononitropyrenes. Recl. Trav. Chim. Pays-Bas 106, 120–128.

Vicente, E.D., Vicente, A.M., Bandowe, B.A.M., Alves, C.A., 2016. Particulate phase emission of parent polycyclic aromatic hydrocarbons (PAHs) and their derivatives (alkyl-PAHs, oxygenated-PAHs, azaarenes and nitrated PAHs) from manually and automatically fired combustion appliances. Air Qual. Atmos. Health 9, 653–668.

Walgraeve, C., Demeestere, K., Dewulf, J., Zimmermann, R., Van Langenhove, H., 2010. Oxygenated polycyclic aromatic hydrocarbons in atmospheric particulate matter: molecular characterization and occurrence. Atmos. Environ. 44, 1831–1846.

Wang, J.Z., Xu, H.M., Guinot, B., Li, L.J., Ho, S.S.H., Liu, S.X., Li, X.P., Cao, J.J., 2017. Concentrations, sources and health effects of parent, oxygenated- and nitrated-polycyclic aromatic hydrocarbons (PAHs) in middle-school air in Xi`an, China. Atmos. Res. 192, 1–10.

Wei, C., Han, Y., Bandowe, B.A.M., Cao, J., Huang, R.J., Ni, H., Tian, J., Wilcke, W., 2015. Occurrence, gas/particle partitioning and carcinogenic risk of polycyclic aromatic hydrocarbons and their oxygen and nitrogen containing derivatives in Xi`an, central China. Sci. Total Environ. 505, 814–822.

Wei, S., Huang, B., Liu, M., Bi, X., Ren, Z., Sheng, G., Fu, J., 2012. Characterization of $PM_{2.5}$-bound nitrated and oxygenated PAHs in two industrial sites of South China. Atmos. Res. 109–110, 76–83.

Wu, Y., Li, G., Yang, Y., An, T., 2019. Pollution evaluation and health risk assessment of airborne toxic metals in both indoors and outdoors of the Pearl River Delta, China. Environ. Res. 179, 108793.

Yang, X.Y., Igarashi, K., Tang, N., Lin, J.M., Wang, W., Kameda, T., Toriba, A., Hayakawa, K., 2010. Indirect- and direct-acting mutagenicity of diesel, coal and wood burning-derived particulates and contribution of polycyclic aromatic hydrocarbons and nitropolycyclic aromatic hydrocarbons. Mutat. Res. Gen. Tox. En. 695, 29–34.

Zhang, D., An, T., Qiao, M., Loganathan, B.G., Zeng, X., Sheng, G., Fu, J., 2011. Source identification and health risk of polycyclic aromatic hydrocarbons associated with electronic dismantling in Guiyu town, South China. J. Hazard. Mater. 192, 1–7.

Zhang, J.M., Yang, L.X., Mellouki, A., Chen, J.M., Chen, X.F., Gao, Y., Jiang, P., Li, Y.Y., Yu, H., Wang, W.X., 2018. Atmospheric PAHs, NPAHs, and OPAHs at an urban, mountainous, and marine sites in Northern China: molecular composition, sources, and ageing. Atmos. Environ. 173, 256–264.

Zimmermann, K., Atkinson, R., Arey, J., Kojima, Y., Inazu, K., 2012. Isomer distributions of molecular weight 247 and 273 nitro-PAHs in ambient samples, NIST diesel SRM, and from radical-initiated chamber reactions. Atmos. Environ. 55, 431–439.

Zimmermann, K., Jariyasopit, N., Massey Simonich, S.L., Tao, S., Atkinson, R., Arey, J., 2013. Formation of nitro-PAHs from the heterogeneous reaction of ambient particle-bound PAHs with $N_2O_5/NO_3/NO_2$. Environ. Sci. Technol. 47, 8434–8442.